

Testing, Development, and First Results of a Method for Measurement of the Isotropy of the One-Way Speed of Light.

May 12th 2017

Gabriel Nowak
Oregon State University

Advisor: Bogdan Wojtsekhowski
Thomas Jefferson National Accelerator Facility (JLab)

1 Abstract

The standard model (SM) of particle physics describes many of the experimentally observed sub-atomic particle interactions. However, there are a few discrepancies with the SM namely: matter/anti-matter asymmetry and dark energy. A current extension of the SM allows for small amounts of Lorentz Violation to fix these discrepancies. Lorentz Violating terms in the standard model extension allow for a small spatial dependence of the speed of light measurable to terrestrial laboratories as a time variation in the speed of light. We present the testing and development of a novel method for measuring the anisotropy of light[1], using the CEBAF accelerator at JLab. Variations in the electron beam's momentum are measured at the entrance and the exit of a magnetic arc, and their ratio is then plotted versus time. Time variations in this ratio correlate to a possible time variation in the one-way speed of light. A preliminary version of the method, only accounting for the largest magnets in ARC1 of CEBAF, measures the isotropy of the one-way speed light to be less than 10^{-11} or one part in 100 billion, which is less precise than the current recorded value of 10^{-14} . We expect to be able to reach better than 10^{-14} levels of precision in future studies with this method.

2 Acknowledgments

Many people whose contributed to the following experiment and hence made this undergraduate thesis possible. First, Heidi Schellman, for her mentorship and programming/academic/life advice. She has always been willing to help with any questions that I may have, and I am grateful for that. Yves Roblin played a very large role in the development of the programs used in this project. Most of the underlying scripts are of his design. I learned a lot about programming while working with him. I would also like to acknowledge Barack Schmookler for his work in developing programs for this project along with ROOT plotting assistance. The assistance from Michael and Francesco at JLab in helping to identify problems in the analysis scripts is much appreciated. I would also like to thank Bogdan Wojtsekhowski who guided me through my internship over the summer and through this project as a whole. His continued patience with me on this project, willingness to discuss confusing concepts, and belief that I could actually complete this project have all been much appreciated. Lastly, I would like to thank many of people I met at JLab including Brian, Abdul, Parker, and Jesse who made the internship recreational as well as educational.

Contents

1	Abstract	1
2	Acknowledgments	2
3	Introduction	5
3.1	Motivation and Objective	5
3.2	The CEBAF Accelerator	5
3.3	Beam Position Monitors	6
3.4	Preface	8
3.4.1	One-Way vs Two-Way Speed of Light	8
3.4.2	Method of Measurement	9
4	Theory	9
4.1	Experimental Theory	9
4.2	The Method of least Squares	11
5	Methods	12
5.1	Overview	12
5.2	Event Data	13
5.3	Optics Data	14
5.4	Root Script	15
6	Data Analysis	17
6.1	Overview	17
6.2	Physical Cuts on Data	17
6.3	BPM Analysis	19
7	Results	23
8	Conclusion	26
8.1	Overview	26
8.2	Future Work	26
9	Appendix	29
9.1	Large Figures	29
9.2	Script Overview	31

List of Figures

1	Cross section diagram of a Beam Position Monitor.	7
2	Side view diagram of a Beam Position Monitor.	7
3	Diagram depicting the difference between the One-Way and Two-Way speeds of light. . .	8
4	Geometric diagram of a magnetic ARC in CEBAF.	10
5	A Flowchart describing the data collection process of the experiment.	12
6	Average readout of BPM data over a one hour period.	13
7	Histogram of $\frac{p_A}{p_B}$ collected over twenty four hours.	16
8	$\frac{p_A}{p_B}$ plotted versus time over a twenty four hour period.	16
9	One dimensional histogram of $\frac{p_A}{p_B}$ over a four day period without a BPM cut.	19
10	One dimensional histogram of $\frac{p_A}{p_B}$ over a four day period with a BPM cut.	19
11	Visualization of beamline including a magnet leading into a BPM.	20
12	Visualization of a beamline including a BPM leading into magnet.	20
13	A "bad" BPM readout versus time.	21
14	Two profile histograms of $\frac{p_A}{p_B}$ comparing the effects of including a "bad" BPM.	22
15	Two dimensional profile histogram of $\frac{p_A}{p_B}$ depicting the final dataset.	23
16	One dimensional histogram of $\frac{p_A}{p_B}$ fitted to a guassian.	24
17	Data from Figure 15 fitted to a sine wave with period of one day.	25
18	Diagram of the CEBAF Accelerator.	29
19	Diagram of the magnets and BPMS in ARC1 of the CEBAF accelerator.	30
20	Overview of the computation process.	31

3 Introduction

3.1 Motivation and Objective

The constancy of the speed of light is one of the most fundamental concepts of physics. Many useful quantities such as the relativistic gamma factor, our definition of SI units, and even the hyperfine structure constant in quantum mechanics are all based upon the speed of light, c . Einstein's postulate, states that the speed of light is constant in all reference frames [12], and a direct corollary is that the speed of light should be non-directionally dependent (anisotropic). Or, the speed of light should be equivalent if measured in one direction as opposed to another. I then present a thesis detailing the testing and analysis of a novel method of measuring the anisotropy of the speed of light [1],[12].

Of further physical interest is the ability of this experiment to test the Standard Model Extension (SME) theory [11]. The standard model is an important theory in the field of particle physics, which governs the interactions of sub-atomic particles as they achieve high energies. Experimental particle physicists can test this theory by colliding sub-atomic particles in large accelerators and using the collision to determine parameters predicted by the standard model. However, there are still some faults with the standard model as it fails to predict antimatter/matter asymmetry, dark energy, and accurate decay rates of certain interactions [8],[9]. The standard model extension was created to try and repair the standard model. This extension to the SM allows for small amounts of Lorentz violation, or a directional dependence on the speed of light. A terrestrial laboratory on earth rotates around the sun. As the laboratory rotates an observer would experience a slight time dependence in the one-way speed of light, indicating a possible directional dependence in this parameter. The experiment described in this thesis is designed to test for a time variation in the speed of light, in order to find evidence of Lorentz violation.

3.2 The CEBAF Accelerator

This experiment takes place at Thomas Jefferson National Accelerator Facility (JLab) in Newport News, Virginia. JLab uses the CEBAF (Continuous Electron Beam Facility) accelerator to conduct medium energy nuclear physics experiments. A working knowledge of the accelerator is required to understand the experiment, and a brief overview of the accelerator is given in this section. See Figure 19 in the appendix for the general layout of the accelerator. The CEBAF accelerator is a racetrack accelerator with two linear accelerators and ten magnetic arcs. It accelerates electrons from < 500 keV/electron to roughly 12 GeV/electron. Please note that these velocities are given as the energy per electron. This is common in accelerator physics as the velocity of the electrons in the accelerator is well within the relativistic region. The definition of special relativistic energy for the electron in the lab frame $E = mc^2\gamma$ relates the two, where m is the mass of the electron and $\gamma = \frac{1}{\sqrt{1-\frac{v^2}{c^2}}}$.

The electron beam begins by shining a laser onto a photoelectric cathode, knocking electrons off of the cathode. The electrons are then accelerated through a small linear accelerator until they are injected into the main machine. Electrons are injected into the larger accelerator at < 500 keV and are first accelerated in the north Linear Accelerator (Linac) before being bent by the first magnetic arc. Each Linac will add between 500 MeV and 1,000 MeV to the beam energy. After ten runs through the two Linacs the beam has roughly 12 GeV of energy. The beam is then ready to be sent to any of the four experimental halls where nuclear physics experiments are set up to accept and manipulate the beam. This experiment does not take place in any of the experimental halls; instead past accelerator data is analyzed. The "continuous" part of the CEBAF acronym makes the CEBAF accelerator a unique accelerator for any physics experiment. While most accelerators use bunches of particles that are a few nanoseconds apart from each other (once length contraction is taken into account) CEBAF uses bunches that are only a few picoseconds away from each other. The effect is that CEBAF produces more electrons and consequently more data faster than a comparable accelerator of a different type.

The CEBAF accelerator has four modes of operations numbered zero through three. A mode of operation indicates "how" or "why" the accelerator is running at a certain time. A beam mode of zero indicates the accelerator is not accelerating electrons. While the electronics of the accelerator may still be, on there are no electrons being accelerated or sent to the experimental halls. A beam mode of three indicates that the accelerator is in continuous wave (CW) mode. This is the optimal mode for data taking as the accelerator delivers a very a stable quality of beam to the experimental halls. Beam modes of one and two indicate other modes of operations such as engineering and maintenance. Data taken during these modes of operation should not be used.

3.3 Beam Position Monitors

A Beam Position Monitor or BPM is an electronic device placed within the beam line of a charged particle beam to measure the position of the center of charge (CoC) of the particle beam. The BPMs used in this experiment do not affect the beam in any meaningful way when measuring the CoC. This is called non-destructive measurement. These BPMs use four separate sensors to detect the location of the CoC. Specifically the impedance of each of the sensors is affected by the proximity of the CoC. For example, when the particle beam is close to a sensor it may have a very low impedance. By comparing the impedances from the four different sensors a BPM can model the position of the CoC within the particle beam. This is useful information as current in the electron beam at JLab follows a gaussian distribution from the CoC. Thus if the CoC is known then the effective position and cross sectional area of the beam is known.

Most BPMs measure the transfer impedance of their four sensors to determine the position of the CoC. The transfer impedance is defined as the ratio between the induced pickup voltage across the

BPM and the beam current at a specific frequency $Z_t(\omega) = \frac{V_p}{I_b(\omega)}$. It should be noted that as the beam current increases so to does the pickup voltage across the BPM. For the purposes of this thesis, the actual calculation of the impedance is not so important as a general understanding of how a BPM works. Further information on calculating impedance can be found in reference [5],[6].

An explanation of how a BPM measures the CoC of a particle beam will be given here. A cross sectional diagram of a BPM is shown in Figure 1, which may be helpful for visualization. Note that in Figure 1 the antennas are rotated forty five degrees from the normal X,Y plane. In order to calculate the position of the CoC in the x' and y' coordinates a standard "difference over sum" method. Where the signal strength of a sensor is dependent on its transfer impedance. In this method the position of the CoC for the particle beam in a specific direction can be found by comparing the signal strength at a positive sensor and negative sensor. For example, to determine the position of the CoC in the x-direction subtract the signal strength in the positive x-direction from the signal strength in the negative x-direction over the sum of the two signals. There is a multiplicative constant that depends on the specific type of BPM being used. Looking at Figure 1 the position in the X' and Y' directions can be calculated as:

$$X' = \frac{1}{S_x} \frac{B - C}{B + C} \quad \text{and} \quad Y' = \frac{1}{S_y} \frac{A - D}{A + D}$$

Once the X' and Y' directions positions have been calculated a rotation must be applied to find the X and Y positions. Equation (1) describes the rotation matrix.

$$\begin{bmatrix} X' \\ Y' \end{bmatrix} = \frac{1}{\sqrt{2}} \begin{bmatrix} 1 & -1 \\ 1 & 1 \end{bmatrix} \begin{bmatrix} X' - X'_{offset} \\ Y' - Y'_{offset} \end{bmatrix} \quad (1)$$

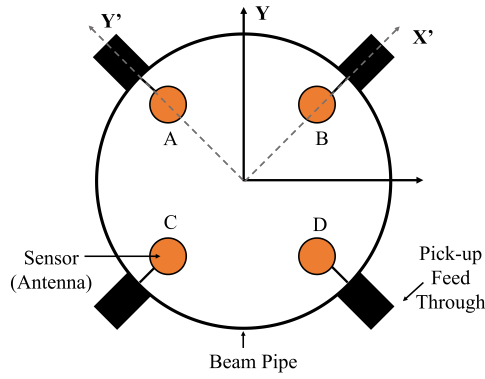


Figure 1: Cross section diagram of a standard BPM in a magnetic arc of the CEBAF accelerator.

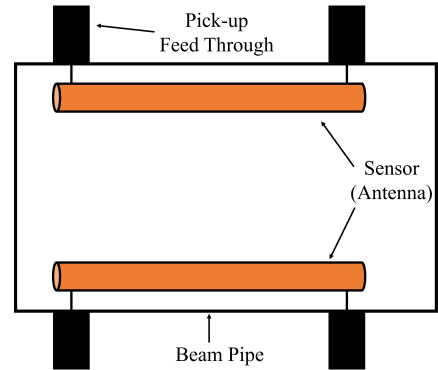


Figure 2: Side view diagram of a standard BPM in a magnetic arc of the CEBAF accelerator.

Many times BPMs will be calibrated to a preferred orbit. In this way a beam that passes exactly through the center of a BPM can read zero for the beam position in the x-direction and y-direction; which is easy to interpret. The X'_{offset} and Y'_{offset} in Equation (1) are used to calibrate the BPMs to this preferred orbit. While very useful, this tuning causes a problem for this method that will be solved in the data analysis section but introduced now. The raw current amplitude of a BPM is a measure of how much the BPM is affected by a particle beam in either the X or Y direction. If a beam is perfectly on center, a beam will record zero current amplitude which is the same reading as if there were no electrons in the accelerator.

3.4 Preface

Before going into the theory of the experiment, a few commonly made misconceptions should be confronted. First, this experiment is not an interferometry experiment. While both types of experiments do measure properties light, they are fundamentally different. Second, the goal of the experiments is to measure a property of light; but the physical measurement tool is actually electrons in the CEBAF accelerator.

3.4.1 One-Way vs Two-Way Speed of Light

There are two characteristics of the speed of light: the one-way and the two-way. The one-way speed of light is the speed associated to light that has only traveled in one direction. The two-way speed of light is the average speed associated to light that has traveled in two directions, normally forward and backward. Interferometry experiments such as LIGO are sensitive to the two-way speed of light, and this experiment is sensitive to the one-way speed of light. The different methods of measuring the speed of light have different limits on their anisotropies (directional-dependence). The two-way speed of light has an isotropy currently bounded at 10^{-18} [2], while the one-way speed of light has an isotropy currently bounded at 10^{-14} [3]. The project described in this thesis measures the one-way speed of light and is not an interferometry experiment.

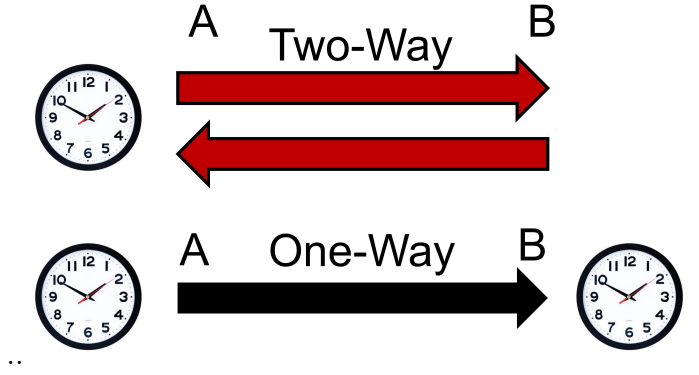


Figure 3: Diagram describing the difference between One-Way and Two-Way speeds of light. Measuring the one-way speed of light means light has traveled in one direction. Measuring the two way speed of light means the light has traveled in two different directions.

3.4.2 Method of Measurement

A common subject of confusion is what this experiment actually measures. While the goal of the experiment is to measure an upper bound on the isotropy of the one-way speed of light; light is not directly involved in any experimental way. Electrons are the physical measurement tool for this experiment. Einstein also postulated that no matter can travel faster than the speed of light. Electrons are a recognized form of matter, and are thus bounded in their speed by the speed of light. In the CE-BAF accelerator, an electron's velocity asymptotically approaches the speed of light. If the one-way speed of light were to "wobble" with respect to time, then a corresponding "wobble" in the speed of the electrons could be measured. Furthermore, if there were some directional dependence (isotropy) to the speed of light then an earthbound laboratory would measure a time dependence in the one-way speed of light; from the earth rotating about the sun. In this way the experiment uses electrons to measure the isotropy of the one-way light.

4 Theory

4.1 Experimental Theory

The result of reference [4] suggests that the isotropy of the one-way speed of light less than 10^{-14} . A terrestrial observer on Earth would experience a possible isotropy of the one-way speed of light as a time variation in the one-way speed of light; corresponding to the preferential direction of the one-way speed of light. More specifically, an observer on earth would experience a sinusoidal variation in the one-way speed of light with a period of one day. So, the signal of interest is a sinusoidal time variation in the one-way speed of light with an amplitude of roughly 10^{-14} and a period of roughly one day. It should be noted that on earth, we are only sensitive to a possible isotropy in the one-way speed of light in a direction perpendicular to the axis of Earth's rotation. So, we define a parameter A being the amplitude of the sinusoidal signal in terms of the measured one-way speed of light (c_a) and the average one-way speed of light (\bar{c}).

$$A = \frac{\bar{c} - c_a}{\bar{c}} \quad (2)$$

To measure the isotropy of the one-way speed of light the relative speed of the electrons in the CE-BAF accelerator is compared to the speed of light: $\frac{c-v}{c}$. Where v is the speed of the electron in the accelerator. A differential δ is applied to identify any changes in this quantity: $\frac{\delta(c-v)}{c}$. Using the linearity of the operator $\frac{\delta(c-v)}{c}$ becomes $\frac{\delta c}{c} - \frac{\delta v}{c}$. Here an important assumption of the experiment is made, that $\frac{\delta v}{c} = 0$. Or that any changes in the velocity of the electrons with respect to the speed of light is "noise" and is not time dependent. This is a fairly safe assumption as the accelerator's ability to accelerate electrons should not change over time; as long as all variables such as external magnetic

fields and maintenance are accounted for. Additionally, electrons do not gain any energy when traveling through the magnetic arcs of the accelerator. Note that the A term defined above is exactly $\frac{\delta(c-v)}{c}$.

Expanding the $\frac{\delta c}{c}$ term yields:

$$A = \frac{\delta(c-v)}{c} = \frac{\delta c}{c} = \frac{\delta \gamma}{\gamma} \frac{1}{\gamma^2} = \frac{\delta R}{R} \frac{1}{\gamma^2} \quad (3)$$

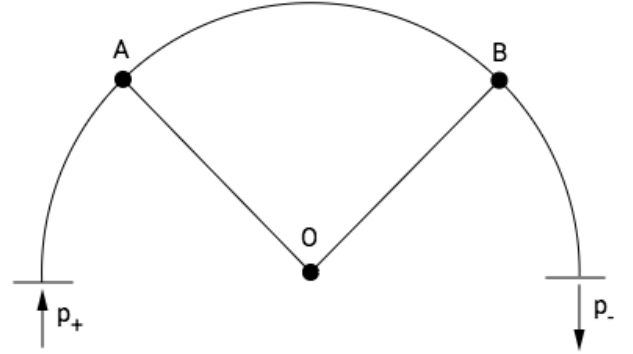
Equation (3) relates the variation in the speed of light to the radius of the electron beam orbit (R) with a scaling factor of γ^{-2} ; where gamma is the Lorentz Factor $\gamma = \frac{1}{\sqrt{1-\frac{v^2}{c^2}}}$. Figure 4 displays a geometric diagram of a magnetic arc in the CEBAF accelerator. In Figure 4 a variation in the beam orbit radius is the difference in length between **OA** and **OB**.

However, the variation in beam orbit radius is not a good measurable quantity as direct measurement is difficult and not allowed. The Lorentz Formula ($R = \frac{Bq}{p}$), from electrodynamics, is used to relate the beam orbit radius to the beam momentum. Where B is the magnetic field that the electron beam is in, q is the net charge of the electron beam, and p is the momentum of the electron beam. In this case B and q are constants and thus are not affected by the δ operator. So, adding an additional equality to Equation (3) yields:

$$\frac{\delta R}{R} \frac{1}{\gamma^2} = \frac{\delta p}{p} \frac{1}{\gamma^2} \quad (4)$$

Equation (4) finally relates a variation in the one-way speed of light to a testable quantity: a variation in the electron momentum from **OA** to **OB** in Figure 4. Of course, the question then becomes how to calculate the deviation in the electron beam momentum. In more formal language, the aim is to calculate the change in momentum (dp) from the nominal momentum (p_0) as the beam enters (dp_A) and exits (dp_B) a magnetic arc. The ratio of these two momenta is taken as a comparison: $(\frac{p_0+dp_A}{p_0+dp_B})$. Momentum is conserved within a magnetic arc so this ratio is expected to be one, with small corrections for energy lost due to synchrotron radiation. Henceforth, any mention of the ratio will refer to:

$$\frac{p_A}{p_B} = \frac{p + dp_A}{p + dp_B} = \frac{1 + \frac{dp_A}{p}}{1 + \frac{dp_B}{p}} \quad (5)$$



..

Figure 4: Geometric diagram of a magnetic ARC in CEBAF. From reference [1].

Equation (5) describes the method of measurement for this experiment. A unique time stamp will then be associated to each $\frac{p_A}{p_B}$ calculation. Then, an analysis of how $\frac{p_A}{p_B}$ varies over time can begin. It should be noted that the deviation(dp) in the beam momentum will be affected by beam stability. Beam stability is a measurement of how stable the beam is over time with respect to position, momentum, angle, and power. Part of the elegance of this method is that the ratio of the momenta is taken, thus any minor changes in beam stability should not affect the outcome of the experiment; because a beam stability should effect both dp_A and dp_B equally. Moving on, to actually calculate $\frac{p_A}{p_B}$, the method of least squares is used.

4.2 The Method of least Squares

The method of least squares is a statistical technique involving the minimization of χ^2 . In this case it is used to fit multiple BPM predictions to the most likely initial conditions (position x , angle x' , and momentum p) of the electron beam. An example will be given below, based on reference [10], for fitting a given set of data to a line ($y = mx + b$).

Suppose that initial data is of the form: $\{(x_1, y_1), (x_2, y_2), \dots, (x_n, y_n)\}$ (6)

We may define the error in fitting this data to a line as: $\chi^2 = \sum_i^n (y_n - (ax_n + b))^2$ (7)

Using the calculus minimization condition: $\frac{\partial \chi^2}{\partial a} = \frac{\partial \chi^2}{\partial b} = 0$ (8)

Evaluating the partial derivatives in (8) and some algebra yields:

$$\begin{aligned} \sum_i^n ax_i^2 + \sum_i^n bx_n &= \sum_i^n x_n y_n \\ \sum_i^n ax_n + \sum_i^n b &= \sum_i^n y_n \end{aligned}$$

The above equations have the form of a matrix, which will be explicitly written below.

$$\begin{bmatrix} \sum_i^n x_i^2 & \sum_i^n x_n \\ \sum_i^n x_n & \sum_i^n 1 \end{bmatrix} = \begin{bmatrix} a \\ b \end{bmatrix} \begin{bmatrix} \sum_i^n x_n y_n \\ \sum_i^n y_n \end{bmatrix} \quad (9)$$

This is known as the least squares matrix, and it can be inverted in order to find the line parameters "a" and "b" that best fit the calculus minimization condition (6). So, by having data about a systems final state the method of least squares can be used to find the most likely initial conditions. Later in this thesis, the method of least squares will be used to calculate $\frac{p_A}{p_B}$.

5 Methods

5.1 Overview

In order to actually calculate a time variation in $\frac{p_A}{p_B}$ a series of ROOT, Perl, and Elegant programming scripts are used to analyze previously collected accelerator data. Figure 5 displays a flow diagram to help visualize the analysis process. First, BPM(event) data are retrieved from the EPICS archiver used by the accelerator division at JLab. Second, optics data from an Elegant script written by Yves Roblin and Barak Schmookler are imported. Optics data is used to calculate transport matrices that represent a magnet's effect on the electron beam. A ROOT script then uses the BPM data and the transport matrices to predict the initial position, angle, and momentum of the electron beam entering and exiting a magnetic arc. Taking the ratio of the two momenta yields $\frac{p_A}{p_B}$, the measurement quantity of the experiment. In order to identify any timelike variations each calculation is assigned a time stamp and graphed versus time. Subsets of the data are excluded before plotting in order to ensure a good quality of data and a physically meaningful relationship.

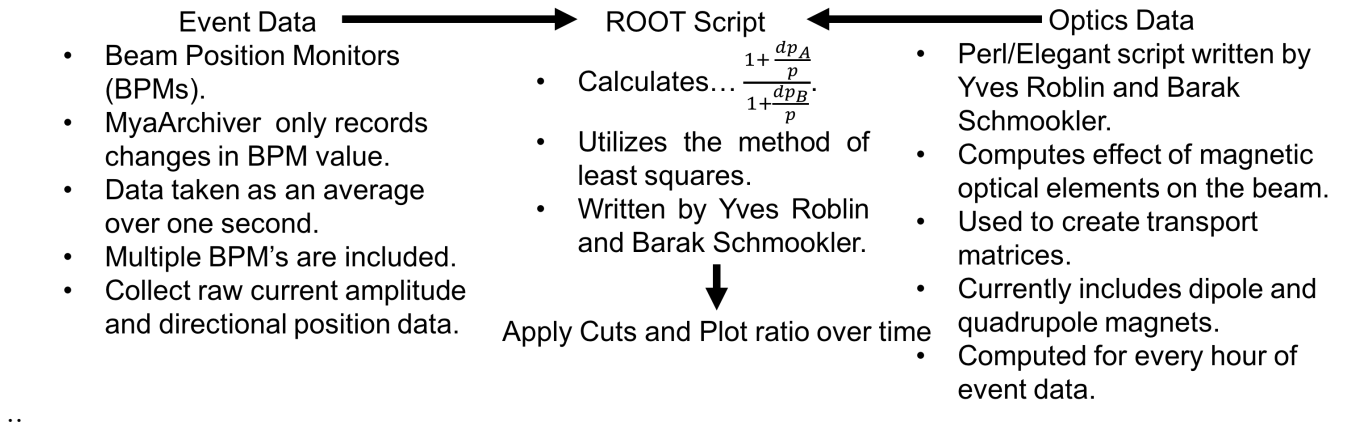


Figure 5: A Flowchart describing the data collection process of the experiment.

5.2 Event Data

Event data is a collection of beam position measurements received from Beam Position Monitors (BPM). It was dubbed “event data” because each $\frac{p_A}{p_B}$ measurement is associated with a time over which BPM measurements were taken. This single calculation is the basic unit of the experiment. It then makes sense to break the long periods of time that an analysis can run over into smaller building blocks, called events.

BPMs are stationed throughout the beamline in the CEBAF accelerator at semi-regular intervals. While there may only be four to five BPMs in the linear accelerator portion of the accelerator, there are around thirty to forty BPMs in each magnetic arc of the accelerator. Beam position data provides a measured final position to predict the initial position, angle, and relative beam momentum at a different point in the beam line. Many BPMs are included in the analysis to improve statistical results. Figure 6 shows a typical readout of a BPM from the EPICS archiver over a one hour period. This specific BPM is in the first magnetic arc of the accelerator, and the beam is relatively stable during this time period. There is a slight glitch at around 25 minutes which is due to the beam being off for a minute or so.

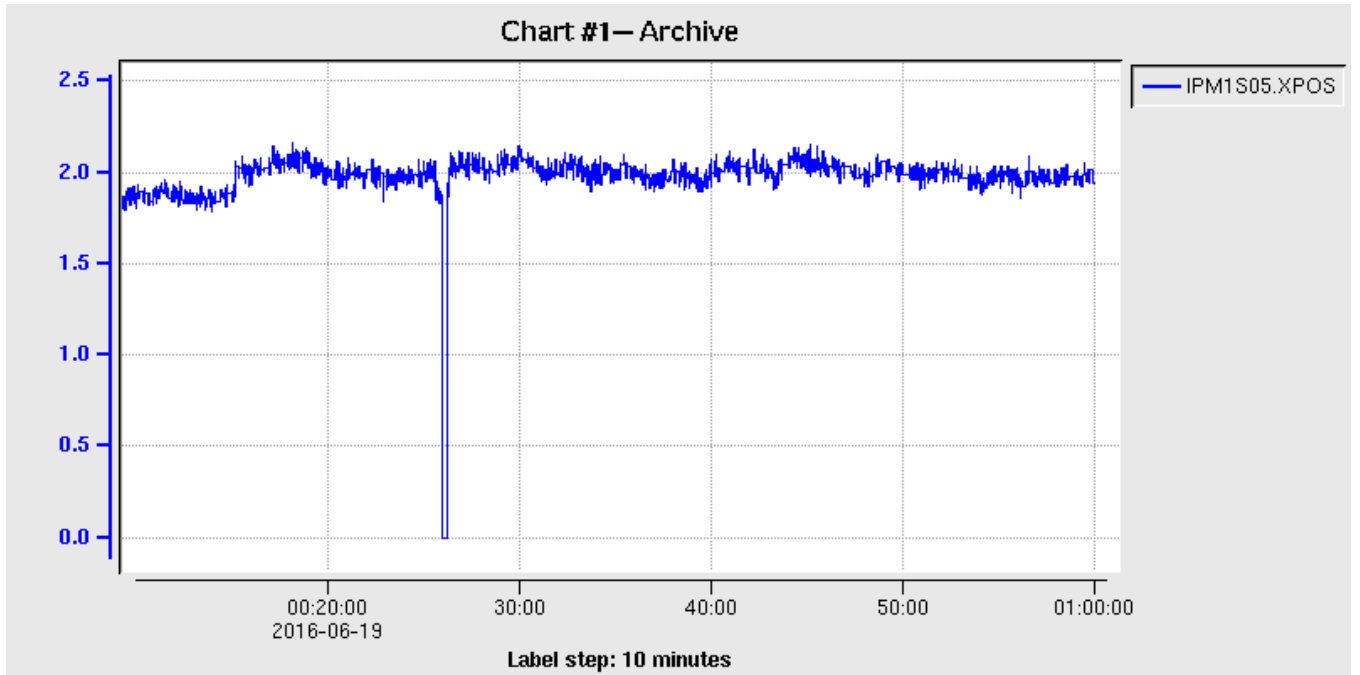


Figure 6: Average readout of BPM data over a one hour period.

These data are stored in the EPICS archiver used by the accelerator division at JLab. An important factor of the EPICS archiver is that the archiver only records changes in measurements. It does not take a measurement at periodic time intervals. This is counter intuitive and opposite to how most archives are structured. One EPICS variable may not change over a period of hours, while a different variable may change on a millisecond basis. For this analysis, data are sampled every second, which makes each event take place over one second. If multiple measurements are taken over a second, the average of these measurements is imported from the EPICS archiver.

5.3 Optics Data

The second type of data required to calculate $\frac{p_A}{p_B}$ is called "optics data." Conceptually, electrons moving in a magnetic arc have an initial position, at the beginning of the arc and a final position, at the end of the arc. Optics data encapsulates the information of what happens to the electron in between the initial position and a final position. More specifically, it represents the effect of magnets on the beamline.

In geometric optics, light entering a prism splits into separate colors depending on the wavelengths present in the incident light. Magnets have a similar effect on a charged particle beam. Charged particles traveling through a magnetic field have their path "bent" by differing amounts depending on their momenta. Higher momenta particles have their path "bent" less than particles with lower momenta. With this a charged particle beam traveling in a magnetic field can be described mathematically by a charged particle having some input coordinate vector, being transformed by the magnet, and having some output coordinate vector. This concept yields itself to be described by a matrix. A charged particle has an initial coordinate vector, and the final position vector can be found by multiplying the initial coordinate vector by a transformation matrix. In one dimension this can be written as:

$$\begin{bmatrix} x_f \\ x'_f \\ \delta \end{bmatrix} = \begin{bmatrix} M_{11}^f & M_{12}^f & M_{13}^f \\ M_{21}^f & M_{22}^f & M_{23}^f \\ M_{31}^f & M_{32}^f & M_{33}^f \end{bmatrix} \begin{bmatrix} x_i \\ x'_i \\ \delta \end{bmatrix} \quad (10)$$

Where x denotes a position, x' denotes an angle, and δ denotes the momentum all with respect to the designed position, angle, and momentum of the beam. To be sure this δ found in Equation (10) is not a differential as found in Equations (3) or (5). It should be noted at this point the transport coefficients (M_{ij}^f) and the final position (x_f) are the only known quantities in Equation (10). As such Equation (10) is not a solvable matrix equation. Equation (11) gives an example of the transport matrix of a particle beam headed aimed directly into a quadrupole magnet of length l . In Equation (11), k depends on the charge and momentum of the incident particles as well as the magnetic field of the quadrupole magnet. More information on this example and magnetic optics can be found in [7].

$$\begin{bmatrix} x_f \\ x'_f \\ \delta \end{bmatrix} = \begin{bmatrix} \cos(\sqrt{k}l) & \frac{1}{\sqrt{k}} \sin(\sqrt{k}l) & 0 \\ -\sqrt{k} \sin(\sqrt{k}l) & \cos(\sqrt{k}l) & 0 \\ 0 & 0 & 1 \end{bmatrix} \begin{bmatrix} x_i \\ x'_i \\ \delta \end{bmatrix} \quad (11)$$

Optics data are used to calculate the transport coefficients in Equation (10). The coefficients are generally dependent on the momentum, angle, and position of the incoming particle as well as the shape and current of the magnet the particle is traveling through. The current inside of a magnet can change from one second to the next and so optics data must be refreshed frequently in order to create accurate matrices. On average, the current inside a large magnet remains relatively constant for a given hour. This analysis calculates optics data every hour on the assumption that the current within large magnets does not change much within a given hour.

Of course, there is more than one magnet in a beam line. Within each arc of the accelerator there are more than 80 magnets ranging from large bending dipoles to smaller diagnostic quadrupoles. Each magnet must be modeled in the optics script to get a good estimate of the initial position, angle, and momentum deviation of the beam. Fortunately, this is done by convoluting the matrices of each individual magnet. So the entire matrix to model an electron traveling through a one hundred and eighty degree arc is the convolution of each individual matrix representing each individual magnet. In this first analysis, only the large bending dipoles were accounted for in the optics script. The smaller focusing dipoles are ignored in this version.

5.4 Root Script

Once both the event and optics data have been imported, the ROOT script can then calculate $\frac{p_A}{p_B}$. From Equation (10), a final coordinate vector in the beamline can be expressed as a transport matrix acting on an input coordinate vector. Taking the first row of Equation (10):

$$x_f = M_{11}^f * x_i + M_{12}^f * x'_i + M_{13}^f * \delta \quad (12)$$

Where the x_f denotes the final position of the beam. Experimentally, x_f is the reading from a single BPM. Each BPM carries information on where the beam is at a specific point in time. In this equation δ , the deviation from the designed momentum, is the desirable quantity as earlier Equation (5) relates $\frac{p_A}{p_B} = \frac{1 + \frac{dp}{p} A}{1 + \frac{dp}{p} B}$. From Equation (12) the error in describing x_f as above is:

$$\chi^2 = \sum_f (x_f - M_{11}^f * x_i - M_{12}^f * x'_i - M_{13}^f * \delta)^2 \quad (13)$$

Applying the method of least squares to Equation (13) calculates the x_i, x'_i , and, δ which minimizes the error in (12). The coordinate vector that the method least squares yields must be the initial position of the electron beam in the magnetic arc. This result can be checked experimentally, as there is a BPM at the beginning of each magnetic arc measuring the beam position. Using this method the momentum deviation(dp) of the electron beam can be found for any point in the beamline. The ratio of these two momenta is then calculated yielding $\frac{p_A}{p_B}$. Figure 7 displays the output of the ROOT script, a one-dimensional histogram of $\frac{p_A}{p_B}$ in ARC1.

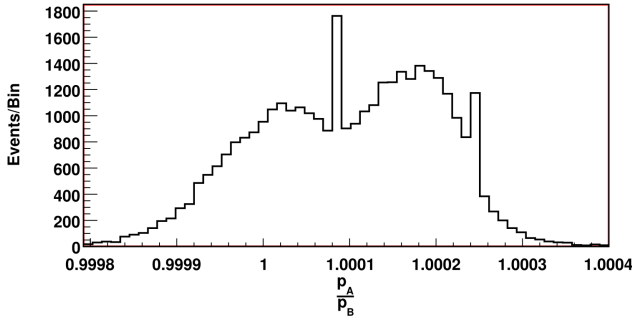


Figure 7: Histogram of $\frac{p_A}{p_B}$ collected over twenty four hours.

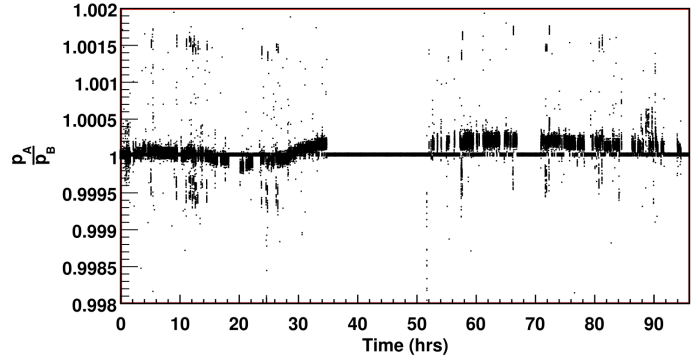


Figure 8: $\frac{p_A}{p_B}$ plotted versus time over a twenty four hour period.

To identify how this ratio varies over time, a time stamp is associated to each individual ratio calculation. Recall that each event takes place over one second. Currently the analysis runs over twenty four hour periods. Since there are 86,400 seconds in twenty four hours, each event is assigned a number between 0 and 86,399. A plot of $\frac{p_A}{p_B}$ versus time is displayed above in Figure 8.

After $\frac{p_A}{p_B}$ has been calculated the data needs to be stored for later analysis. The data from the ROOT script is stored in a text file where each row contains data from a single event and is one hundred and ninety one units long, and of the form:

Listing 1: Format of Raw Data output from Root Script.

```
time dp1 dp2 ratio xpos1 xpos2 amp1 amp2 magc
```

Where time is a number ranging from 0 to 86400 that represents the second the beam data was averaged over. dp1,dp2, and ratio are the same as in Equation (5). xpos1 and xpos2 are the position measurements of the front and back BPMs. amp1 and amp2 are the raw current amplitudes in the front and back BPMs. Finally, magc is the raw current in each of the magnets in Arc 1.

6 Data Analysis

6.1 Overview

The data from the ROOT script are raw, and has not been manipulated in any way. The data are not all of a good quality or even corresponds to a physical situation. For example, data are still collected even if the CEBAF accelerator is off (not accelerating electrons). This data clearly does not correspond to a physical situation. Data are also collected if a BPMs measurements fluctuate greatly and impair the analysis. It should be noted that a BPM which records fluctuating measurements is not necessarily incorrect. The data are still quite useful for the beam division at JLAB, it is simply not good data for this experiment. Thus the data needs to be "cleaned" through a series of exclusions colloquially called "cuts". Whenever a "cut" is referenced further in this thesis it indicates an exclusion of a particular subset of data. This section will describe the cuts applied to the raw data to ensure a good quality of physically meaningful data. The first cut applied ensures a physically meaningful data point. In this case that means excluding data points recorded when the CEBAF accelerator is off. Then, a good quality of BPM data must be ensured, as it is the physical quantity used to calculate $\frac{p_A}{p_B}$. There is currently no automated way to ensure the BPMs are working well, so the data are checked manually. If a BPMs readings are found to fluctuate then data are recollected excluding that BPM.

6.2 Physical Cuts on Data

Data points may not correspond to a physically meaningful result for many reasons. The primary reason for this experiment is that the accelerator could be off, but still taking data. While the electronics of the accelerator stay on at all times at JLab, the accelerator is not always accelerating electrons. Reasons for this include maintenance and engineering runs. In either case data are still recorded during these down periods as it is easier to record the data and exclude certain time periods rather than only collect data when the accelerator is in a beneficial mode. The goal of the physical cuts is to only include data when the accelerator is in CW (continuous wave mode). The modes of the accelerator were discussed earlier in the introduction; but the main idea is that when the accelerator is in CW mode it delivers exceptionally stable beam to the experimental halls.

To be sure, including only physically relevant data makes a difference in the results of the experiment, although not in the traditional sense. Normally, the idea of an unrealistic data point is thought of as a wildly insane value that is obviously out of place within a physically meaningful data set. That is not the case here. As stated earlier in the methods section, the goal of the optics script is to account for as many magnets/magnetic fields in the beamline as possible. The expected value of the ratio, $\frac{p_A}{p_B}$ is one. For this experiment, physically meaningless data boils down to meaning that there were no electrons in the accelerator; or that the beam was not stable at the time of a measurement. How-

ever, since the electronics are still powered the BPMs still record a position value. In the case that there are no electrons to effect the measurement of the BPM, the instruments all record 0 for a beam position. To the ROOT script a beam position of zero indicates that the electrons are exactly on their preferred orbit, without any error or deviation ($dp_A = dp_B = 0$). Thus when $\frac{p_A}{p_B}$ is calculated a value of one is received:

$$\frac{p_A}{p_B} = \frac{p + dp_A}{p + dp_B} = \frac{1 + \frac{dp_A}{p}}{1 + \frac{dp_B}{p}} = \frac{1}{1} = 1$$

A $\frac{p_A}{p_B}$ value of one is the expected result from the experiment. Thus when unphysical data is analyzed it yields the expected value. So data sets that include unphysical data points are weighted more to the expected measurement value than data sets with only physical data. This creates an odd version of experimental bias that should be avoided. A cut must then be created to exclude unphysical data points yet keep the physically relevant data points. Currently there does not exist a beam mode variable in the recorded data as it was not included in the original datasets. Furthermore, the data collection program takes roughly 12 hours to run and it would take days to regenerate the data. So, while current on a beam mode variable would best, it was decided that a similar cut would be invented so the data would not need to be regenerated. The first listing in the methods details the available variables to use. The new cut was decided to use the raw current amplitude of the BPMs. The raw current amplitude of a BPM is a measure of how affected the BPM is by the beam position in either the x or y direction. So, for a raw current amplitude to read a zero value the beam must be exactly on target in both the x and y directions. The cut is then defined as if all BPMs in the magnetic arc read raw current amplitude of zero for a single event, the event is excluded. This "raw current amplitude" cut is not exactly the same as a "beam mode" variable cut, and is in fact a larger cut. Meaning that some amount of good data are being excluded.

Figures 9 and 10 display 1-D histograms of $\frac{p_A}{p_B}$ before and after applying the above cut. Note that roughly 100,000 events are excluded, all of which had a $\frac{p_A}{p_B}$ value of 1. This ends up being about 50% of the events collected during this time period. If all 100,000 events were kept in the data sample then the average value of $\frac{p_A}{p_B}$ would be heavily skewed towards one. Which although it is the expected result does not correspond to a physical situation. There are two more reasons why a large peak of $\frac{p_A}{p_B}$ at one does not make sense. First, while the CEBAF accelerator is a well tuned machine, it is not perfect. It is relatively uncommon for an electron beam to be perfectly on the preferred orbit for every single BPM in the magnetic arc. Second, as stated in the methods section this analysis only accounts for the large bending dipoles in the optics script. These large magnetics cannot hope to achieve a perfectly centered beam, so some spread in the $\frac{p_A}{p_B}$ distribution away from one is expected. Thus the exclusion of this data is well justified and has given a reasonable result.

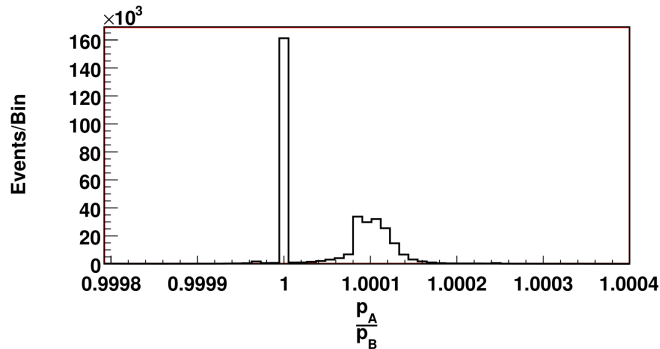


Figure 9: One dimensional histogram of $\frac{p_A}{p_B}$ over a 4 day period. The large peak at one is caused by the accelerator being down for a large time period during the analysis.

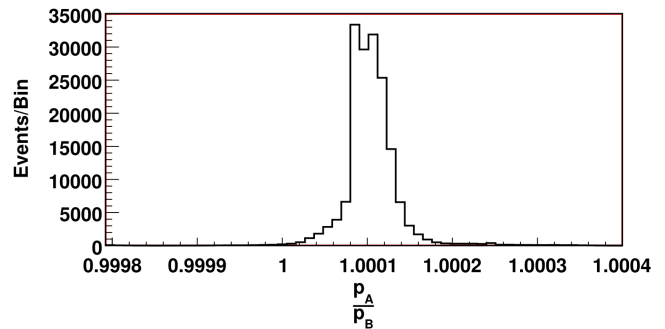


Figure 10: One dimensional histogram of the ratio over the same period as the previous picture, but with a cut on the raw current amplitude of the BPMs. The previous peak at one has been eliminated.

6.3 BPM Analysis

Picking which BPMs are included in the ROOT script's event data is another important data exclusion present in the experiment. At first thought, including or excluding certain BPMs should not directly effect the calculation of $\frac{p_A}{p_B}$. However, there are a few imperfections within the analysis that create a preference for how BPMs are chosen: where the included BPMs are located within the accelerator, how many BPMs are included in the ROOT script, and which BPMs are included all effect the calculation of $\frac{p_A}{p_B}$. In this section I will explain the criterion for how a BPM is included/excluded.

There are forty eight BPMs in ARC1 of the CEBAF accelerator. A criterion for picking a good "BPM" to include in the ROOT script must be created in order ensure a good quality of data. It may be helpful to refer to Figure 18 in the appendix while reading this section for a visualization of where these BPMs are located within ARC1 of the accelerator. First recall that the BPMs are used to calculate the deviation from the nominal momentum of the electron beam about the entrance and exit of a magnetic arc. It is then wise to choose BPMs located at the entrance and exit of the magnetic arc. So, a magnetic arc is split into a "upper" and "lower" half for the purposes of this analysis. The designation is completely arbitrary, here the entrance of the ARC is denoted "upper" for simplicity sake. BPMs that are in the middle region of the ARC (~ 480 - ~ 680 meters) are not included. Immediately, this excludes many BPMs from being included in the ROOT script.

In the methods section of this thesis, it was stated that only the large magnets are currently accounted for in this optics script. There are one hundred and forty seven magnets in ARC1 of the CEBAF accelerator, but only eighty four of these magnets are included in the optics script. The main bending effects of the magnets on the electron beam are taken into account but there are smaller ef-

fects that are currently not being taken into account. Truthfully, there is an easy and a hard way to fix this. Until the hard way is completed (account for every magnet in a magnetic arc in the optics script), the easy way is currently being used. That is, picking BPMs that are heavily effected by smaller magnets. To visualize this, consider the following two cases. In one case, a BPM is placed before a small magnet; and in the other a BPM is placed after a small magnet. See Figures 11 and 12 below for an illustration.

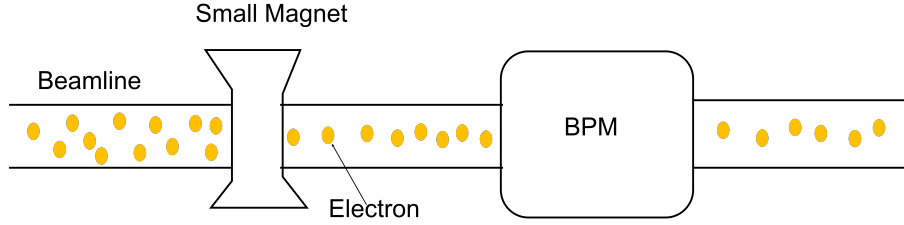


Figure 11: Visualization of a magnet and BPM in the beamline. Note that after the magnet the electron beam is more focused. Since the BPM is placed after the magnet the BPM records this focused beam position.

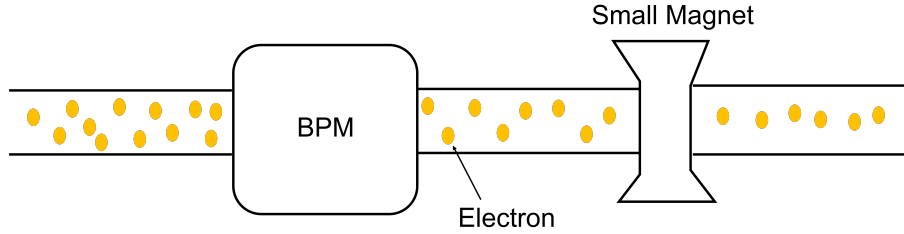


Figure 12: Visualization of a magnet and BPM in the beamline. Note that after the magnet the electron beam is more focused. Since the BPM is before the magnet the BPM records the unfocused beam position.

The main difference between Figures 11 and 12 is that when the BPM is placed after the magnet, the BPM records a focused beam position value. If the BPM is located before the magnet the BPM will record a larger beam position value, as the beam is unfocused. These illustrations show that it is important to use BPMs that are in front of the smaller, focusing magnets. In this way a BPM will account for any push the smaller magnets might give the beam, without actually accounting for the smaller magnets in the optics script. It should be noted that this process can actually happen in reverse. Some magnets are meant to destabilize the beam, and the data is useful for the beam division at JLab.

There are two diagnostic magnets in particular that give the beam a small kick in ARC1: MBTE02H and MBT1S10H. These magnets are often used to give the beam a small push to observe how the deviation propagates through the machine. To avoid the effects of this magnets only BPMs further down the beamline then the two magnets are chosen for use in the ROOT script. The BPMs past MBTE02H and before the four hundred and eighty line are the BPMS included for the "upper" arc. The bottom BPMs, so far, have not had as troublesome of magnets, and thus most BPMS past six hundred and eighty to the end of the arc are included in the ROOT script.

The last important criterion for picking a good BPM are that the BPM readings must to be stable. This remark nearly goes along with the last criterion, except that beam instability is not entirely caused by unruly magnets. In this case it may not be known what causes the beam instability. In order to search for BPM instability, the BPM outputs are periodically manually checked for "bad" readings with respect to this experiment. A bad reading, is a clearly time dependent beam position signal. There should largely be no time dependent behavior in a BPM signal, but some effects are simply not accounted for in this analysis. An example of a bad BPM output is given in Figure 13. Note the oscillatory behavior, of which the period is roughly equivalent to one day.

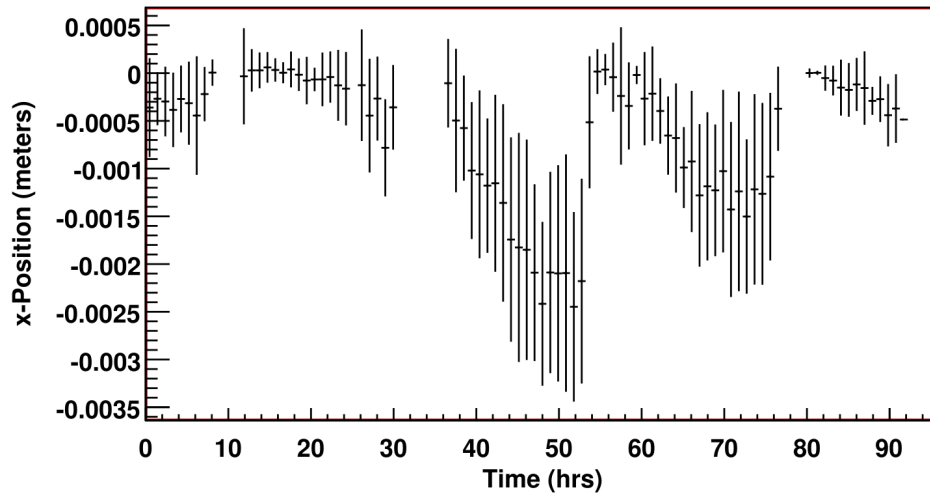


Figure 13: Beam position with respect to the designed position in meters vs time in hours for IPM1A04. Note that there is clear oscillatory behavior with a period of roughly twenty four hours.

The cause of the oscillatory behavior in Figure 13 is unknown, but a reasonable hypothesis would be that some thermal load is effecting the measurement of the BPM. In any case, this oscillatory behavior will have a clear effect on the calculation of $\frac{p_A}{p_B}$. It should be noted that this behavior is not the expected signal, A , even though the oscillations have a period of roughly one day. These oscillations

are not representative of a larger effect because this BPM is the only BPM in the magnetic arc that exhibits this behavior over this time period. Additionally, A would be characterized by much smaller oscillations than measured here.

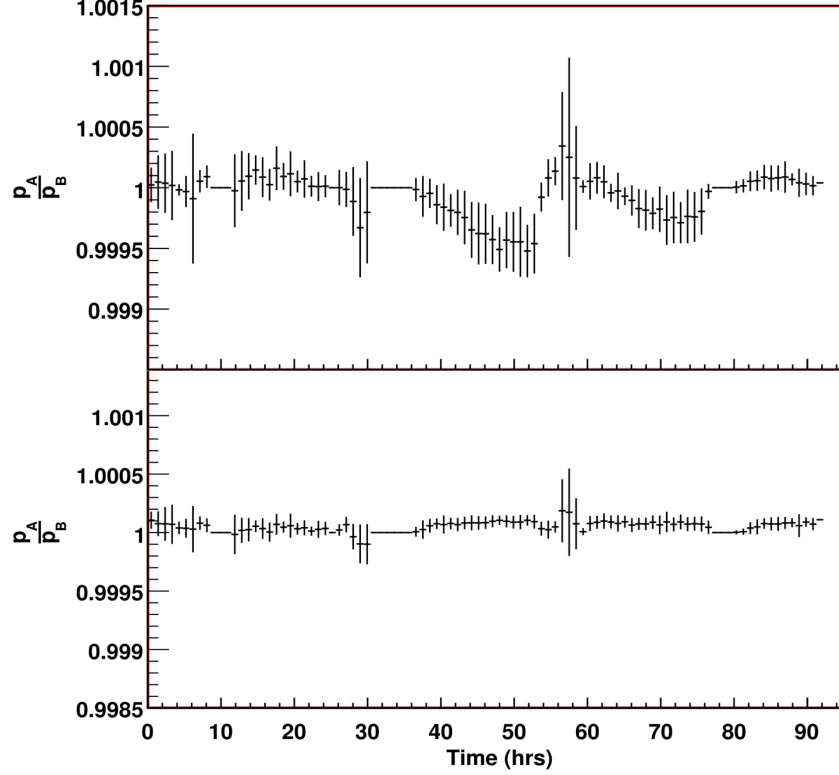


Figure 14: Two profile histograms of $\frac{p_A}{p_B}$ over a four day period. The top histogram was produced with data including a "bad" BPM, while the bottom histogram was produced with data excluding the "bad" BPM. Notice the clear oscillatory behavior in the top histogram, related to Figure 13.

Figure 14 depicts $\frac{p_A}{p_B}$ plotted over the same time period as Figure 13. In it, the effect of the bad "BPM" on the value of $\frac{p_A}{p_B}$ can be clearly identified. The top plot displays $\frac{p_A}{p_B}$ calculated with the "bad" BPM in Figure 13. The bottom plot displays $\frac{p_A}{p_B}$ calculated using data that excludes IPM1A04, the "bad" BPM. Notice that there is clear oscillatory behavior in the upper plot of Figure 14 that nearly matches the behavior of the BPM in Figure 13. Excluding the data from this BPM gives a much cleaner $\frac{p_A}{p_B}$ signal, as shown in the lower plot of Figure 14.

7 Results

Once a good subset of raw data has been isolated, a possible time variance in the one-way speed of light can be calculated. From a roughly 4-day data sample, Figure 15 displays $\frac{p_A}{p_B}$ as a function of time using a two dimensional profile histogram. A profile histogram is a histogram where each bin contains the mean value of its entries. In the following graph, each bin contains the mean value of $\frac{p_A}{p_B}$ for the data in each bin.

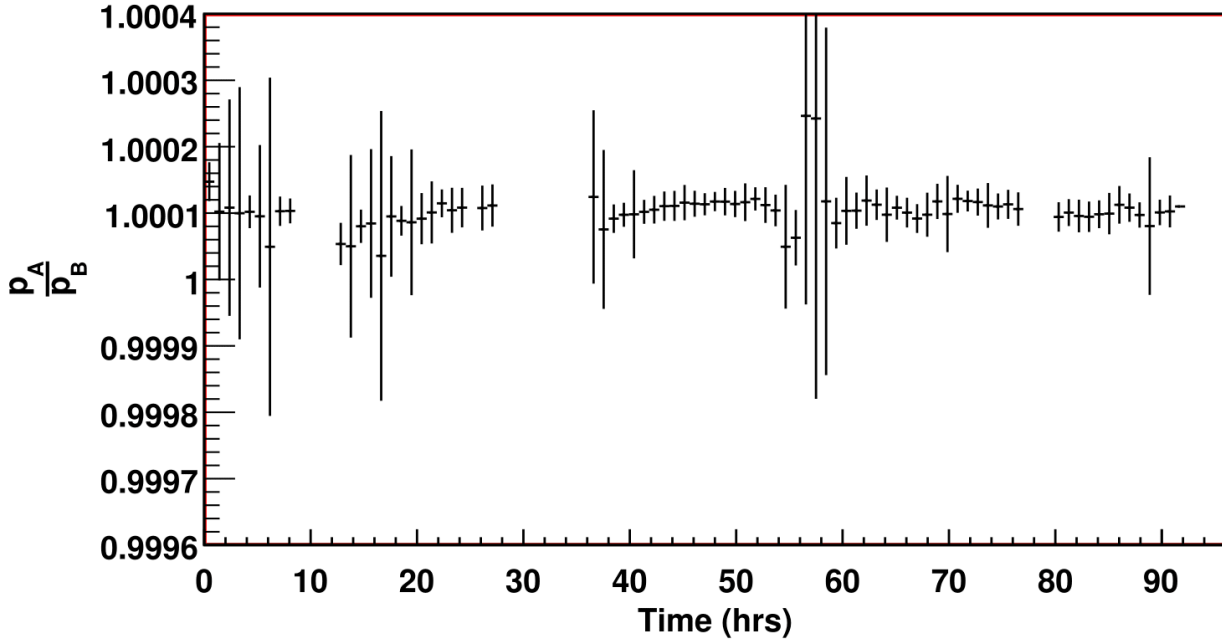


Figure 15: Two dimensional profile histogram of $\frac{p_A}{p_B}$ over a four day period. Note that the ratio is stable on the 10^{-5} level.

Figure 15 displays $\frac{p_A}{p_B}$ versus time over a four day period. The stability of $\frac{p_A}{p_B}$ over time can be related to a possible time variation in the one-way speed of light through Equation (3). Here, stability is defined to mean how closely $\frac{p_A}{p_B}$ oscillates around its' mean value. It is then important to identify the deviation of $\frac{p_A}{p_B}$ from the average $\frac{p_A}{p_B}$ over a time period. From Figure 15, the average value of $\frac{p_A}{p_B}$ seems to be roughly 1.0001, and $\frac{p_A}{p_B}$ can be seen to have stability of roughly 10^{-5} or one part in one hundred thousand to the observing eye. A more quantitative determination of the stability of $\frac{p_A}{p_B}$ will be shown soon.

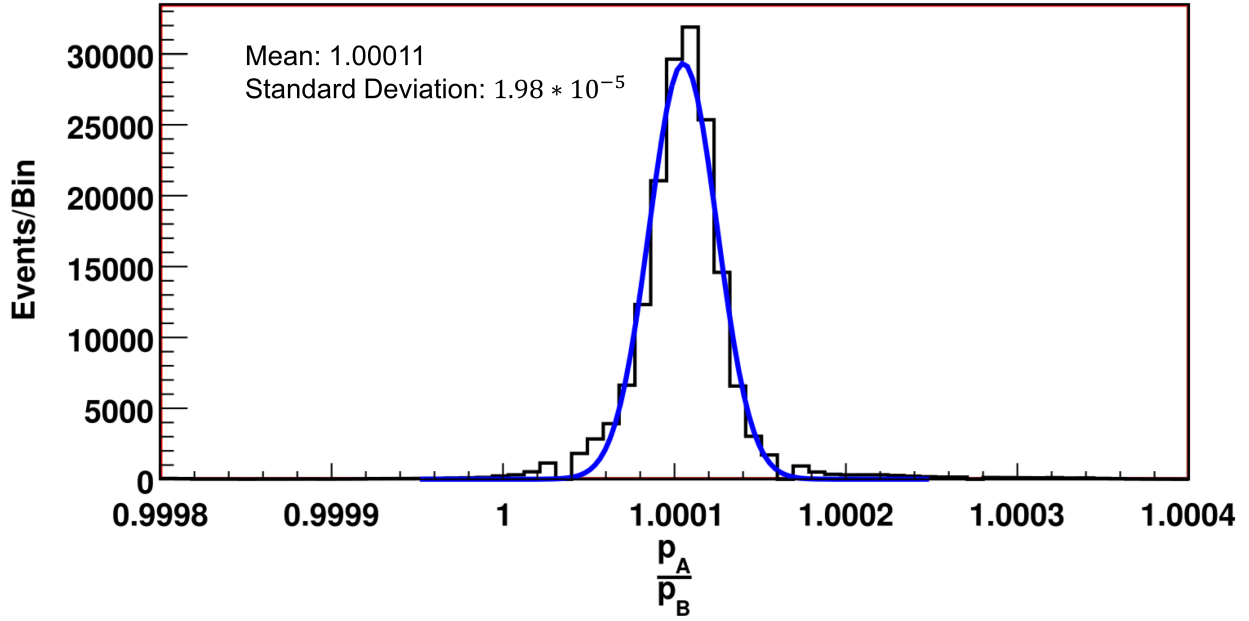


Figure 16: One dimensional histogram of $\frac{p_A}{p_B}$ fitted to a gaussian. The important quantity in this graph is the standard deviation of the gaussian $1.98 * 10^{-5} \pm 5.0 * 10^{-8}$, which is related to the deviation of $\frac{p_A}{p_B}$ over time.

To learn more about the measured $\frac{p_A}{p_B}$, a one dimensional histogram of $\frac{p_A}{p_B}$ over the same time period as Figure 15 is useful. The expected sinusoidal signal of the time variation of the one-way speed of light, $A\gamma^2$ is on the order of 10^{-8} . So, the standard deviation of a gaussian fitted to a histogram of $\frac{p_A}{p_B}$ is expected to be on the order of $\frac{10^{-8}}{\sqrt{2}}$; by relating the RMS of a sine wave to the standard deviation of a gaussian. Finding the one dimensional histogram of $\frac{p_A}{p_B}$ is equivalent to projecting all of the data from Figure 15 onto the y-axis. Figure 16 displays this histogram, fitted to a gaussian function to gain useful statistics about $\frac{p_A}{p_B}$. Most importantly, the fitted gaussian has a standard deviation of $1.98 * 10^{-5}$, which means that $\frac{p_A}{p_B}$ is stable to roughly 10^{-5} . First, 10^{-5} is significantly greater than 10^{-8} so the experiment may not be sensitive to the desired signal on the order of 10^{-8} . In addition, it can immediately be seen that the mean value of $\frac{p_A}{p_B}$ is 1.0001 over this time period, which is a clear shift away from the expected value of one. This shift is most likely caused by not including the effect of every magnet in ARC1 in the optics script. Other, less likely causes include an intrinsic bias in the CEBAF accelerator when accelerating the electrons.

While a one dimensional histogram is useful to gain statistics about $\frac{p_A}{p_B}$, the goal is to identify a time like variation in the one-way speed of light and relate it to the isotropy of the one-way speed of light. Results from reference [4] suggest a possible isotropy in the one-way speed of light that could be measured as a time like variation in the one-way speed of light for a terrestrial laboratory. Specifically, it predicts a sine wave of frequency one day. Actually 23.599 hours due to using sidereal time instead of the standard sun-centered time. Figure 17 depicts the data found in Figure 16 fitted to a sine wave with a set period of one day.

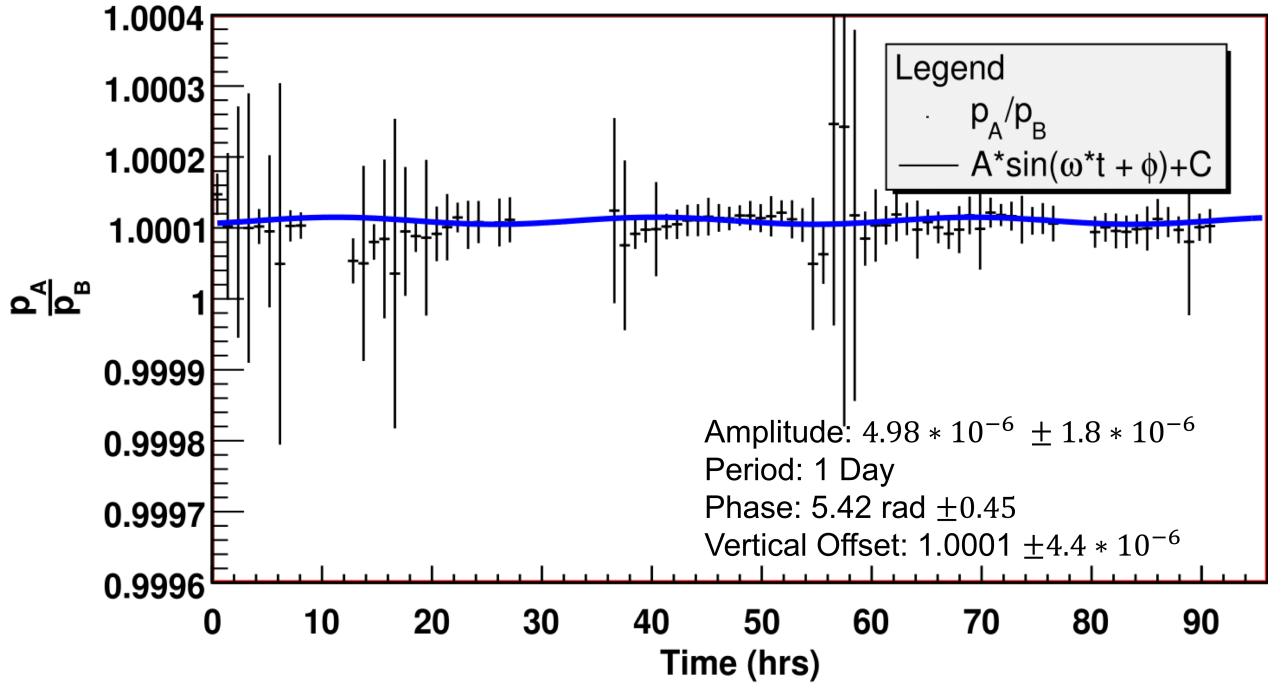


Figure 17: The two dimensional profile histogram of $\frac{p_A}{p_B}$ from Figure 15 fitted to a sine wave with period of one day. The amplitude, describing a possible time variation of the one-way speed of light, is of order 10^{-6} .

Figure 17 depicts the final data from Figure 15 fitted to a sine wave with a period of one day. The amplitude of this sine wave describes the size of a possible time variation in the one-way speed of light. The fit yielded a value of $4.98 \times 10^{-6} \pm 1.8 \times 10^{-6}$ for the amplitude of the sine wave, so a conservative limit on the measured amplitude would be $A_{meas} < 3 \times 4.98 \times 10^{-6} = 1.49 \times 10^{-5}$. As described in the introduction, the time variation of $\frac{p_A}{p_B}$ can be related to $\frac{\delta c}{c}$. Recall an equality from Equation (3):

$$\frac{\delta c - v}{c} = \frac{\delta p}{p} \frac{1}{\gamma^2} = \frac{\delta p_A}{p_B} \frac{1}{\gamma^2}$$

Up to this point the $\frac{1}{\gamma^2}$ factor has been ignored. This analysis was done using data from ARC1, which has a γ factor of roughly 2150 over the time period this data was collected. Using the amplitude of the sinusoidal function as the variance of $\frac{p_A}{p_B}$ a possible time variation in the one-way speed of light can be found using the above equality.

$$\frac{\delta c}{c} = \frac{\delta p}{p} \frac{1}{\gamma^2} \leq 1.49 * 10^{-5} * \frac{1}{2150^2} = 3.23 * 10^{-11} \quad (14)$$

The first observation to make is that 10^{-11} is much greater than the current measurement of 10^{-14} [2]. The experiment is then currently not sensitive to the expected sinusoidal signal, $A \approx 10^{-14}$. More information will be present in the future work section about how this experiment can be used to get closer to the current measured value. While this result yields no indication of any time variation in the speed of light it does indicate that the method described in [1] can feasibly be used to find a possible variation of this type. The uncertainties on each of the fits are due to the statistical uncertainty when converting the raw data into a profile histogram. The experimental uncertainties still need to be calculated at the time of this thesis.

8 Conclusion

8.1 Overview

In conclusion we present the development of a novel method for determining the isotropy of the one-way speed of light. Using the CEBAF accelerator at JLab in Virginia the experiment described in this thesis measures the change in electron beam momentum as the electron beam enters and exits a magnetic arc. This ratio of momenta in the magnetic arc is sensitive to a possible spatial dependence in the one-way speed of light; expected in the case of Lorentz Violation. Through data collections of a four day period, an upper bound for the isotropy of the one-way speed of light on the order of 10^{-11} was measured. This measurement is three orders of magnitude less accurate than the current measurement of 10^{-14} . We expect to achieve better than 10^{-14} levels of precision in future studies with this method.

8.2 Future Work

Looking toward the future this method shows promise in being able to investigate further into the upper bound of the isotropy of the one-way speed of light. This beginning analysis utilized ARC1 of the CEBAF accelerator which has a relativistic Lorentz factor on the order of 10^3 . Each magnetic arc in

the CEBAF accelerator contains consecutively higher energy electrons, and thus larger gamma factors. As an example the gamma factor of ARC10, the highest energy magnetic arc, is on the order of 10^4 . A larger gamma factor would allow for a more precise measurement of the isotropy of the one-way speed of light. However, with the greater precision comes the challenge of accurately modeling higher energy electrons and successfully accounting for larger magnets. Additionally, the method could be improved by simply including more data. The results of this thesis were measured using a four day data sample. Larger amounts of data means a better fit to identify possible time variations. Continuing work on this experiment will include accounting for a greater number of magnets in the optics script, and working to modify the ROOT script for use on higher energy arcs.

References

- [1] Bogdan Wojtsekhowski. *On measurement of the isotropy of the speed of light*. Europhysics Letters. 108-3, 31001(2014).
- [2] M.Nagel *et al.* *Direct Terrestrial Test of Lorentz Symmetry in Electrodynamics to 10^{-18}* . Nature Communications. 6, 8174 EP(2015).
- [3] Y. Michimura *et al.* New Limit on Lorentz Violation Using a Double-pass Optical Ring cavity. Phys. Rev. Lett. 110, 200401.
- [4] J.-P. Bocquet *et al.* Limits on Light-Speed Anisotropies from Compton Scattering of High-Energy Electrons. Phys. Rev. Lett. 104, 241601.
- [5] Chao, Alexander Wu. *Handbook of Accelerator Physics and Engineering: 2nd Edition* (World Scientific Publishing Company, 2013)
- [6] A.S. Hoffer, B.A. Bowling, C.S. Higgins, P.K. Kloeppel, G.A. Krafft, K.L. Mahoney. *Performance of the CEBAF arc beam position monitors*. Particle Accelerator Conference 1993.
- [7] Conte, M. & MacKay, W. W. *An Introduction To The Physics Of Particle Accelerators*. (World Scientific Publishing Company, 2008).
- [8] Lykken, J. D. *Beyond the Standard Model*. arXiv:1005.1676 [hep-ph] (2010).
- [9] BABAR Collaboration et al. *Evidence for an Excess of $\overline{B} \rightarrow D^{(*)}\tau^-\overline{\nu}_\tau$ Decays*. Phys. Rev. Lett. 109, 101802 (2012).
- [10] The Method of Least Squares. Miller, S. Department of Mathematics, Brown University.
- [11] Colladay, D. & Kostelecký, V. A. *Lorentz-violating extension of the standard model*. Phys. Rev. D 58, (1998).
- [12] Einstein, A. *Zur Elektrodynamik bewegter Körper*. Ann. Phys. 322, 891–921 (1905).
- [13] Wojtsekhowski, B. *Study of the one-way speed of light anisotropy with particle beams*. EPJ Web Conf. 142, 01029 (2017).

9.1 Large Figures

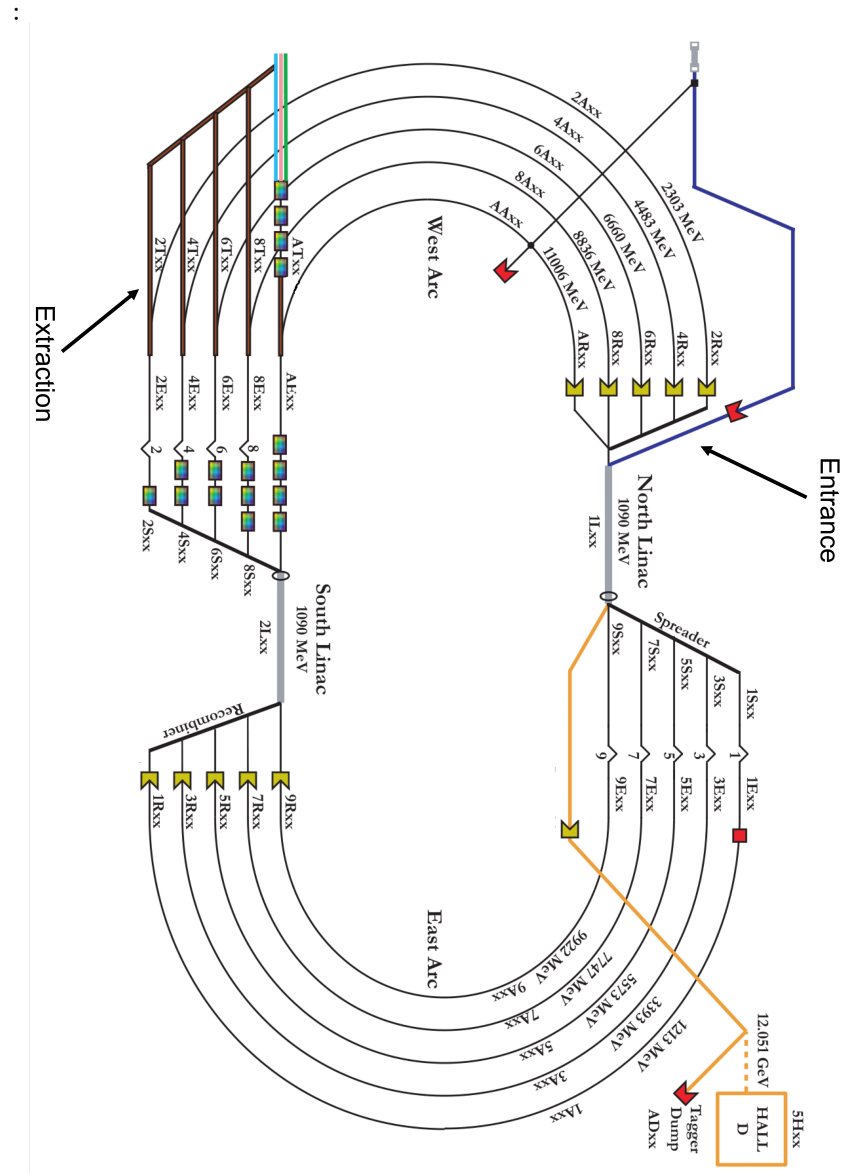


Figure 18: Diagram of the Continuous Electron Beam Accelerator Facility (CEBAF) at Jefferson Lab in Newport News, VA

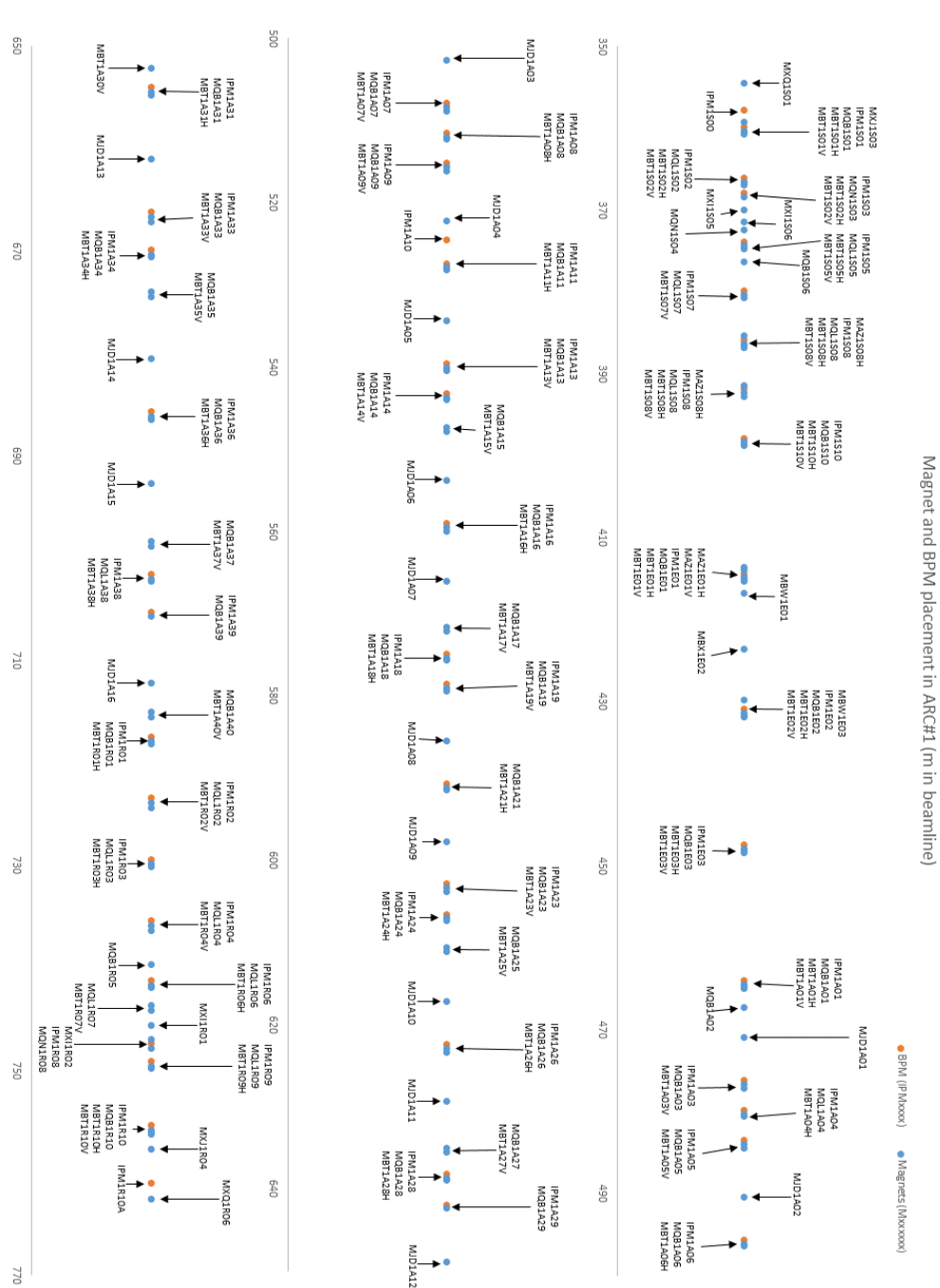


Figure 19: Dsiagram of the magnets and BPMs in ARC 1 of the CEBAF accelerator as a function of distance in the arc.

9.2 Script Overview

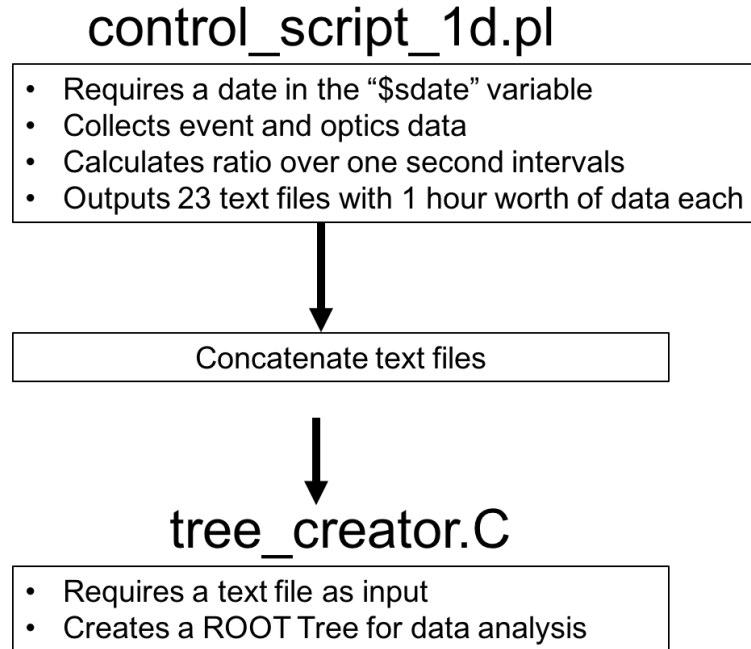


Figure 20: Overview of the computation process.

In the hopes of someone continuing this project I have included this short overview of how to actually use the programs that Yves, Barak, and I have wrote. I do not know the current knowledge of the reader, so I will assume that the reader knows some basic Linux terminal commands. However, I will list the commands and syntax used as well. The goal of this overview is to be able to utilize already existing programs on the operations computer at JLab to create a usable ROOT TTree to analyze c-speed data. First, one must copy the programs from Yves, Bogdan's, or my directory on the JLab accelerator operations computer. The current list of needed programs can be found at the end of this overview.

The first program to run is "control_script_1d.pl". No explicit input is required, but the "\$sdate" variable needs to reflect the day for which one wants to collect data. To change the "\$sdate" variable open "control_script_1d.pl" in a text editor and manually change the value. "\$sdate" should be a string of the form "YEAR-MONTH-DAY". As an example, you may like to analyze August 30th of 2016 "\$sdate" would then be set to the string "2016-08-30". Control_script will then calculate $\frac{p_A}{p_B}$ over that day starting at "00:00:00" and ending at "11:59:59". The $\frac{p_A}{p_B}$ being calculated once every second. The program outputs a text file where each row has the following form:

```
time dp1 dp2 ratio xpos1 xpos2 amp1 amp2 magc
```

Where `dp1` is the difference from the nominal momentum in the beginning of ARC1, `dp2` is the difference from the nominal momentum at the end of ARC1, the `ratio` is our measurement, `xpos1` is an array of the x-position values of the twelve front BPMs, `xpos2` is an array of the x-position values of the eight back BPMs, `amp1` is an array of the raw current amplitude of the front twelve BPMs, `amp2` is an array of the raw current amplitude of the back eight BPMs, `magc` is an array of the current in each of the one hundred and forty eight magnets in ARC1. There should be 86400 rows in the text file as each row represents one second.

"`control_script_1d.pl`" takes roughly twelve hours to run. At least for myself, it is not feasible to leave a command prompt open for twelve hours. As such it may be productive to use the linux "`nohup`" command to exit the command line and still have the program run. Additionally, it is always a good idea to write the output of the program to a text file in order to track its progress. The most common usage is as follows:

```
nohup ./control_script_1d.pl > log.txt &
```

Once the program has completed, twenty three new text files will be in the same directory as "`control_script_1d.pl`". These text files will have the form "`MonthDay_hourstarted_lengthoftime_specialcharecter`". An example is "`0830_1200_1h_A01.txt`". This would be a text file containing data from August 30th containing data from "`12:00:00`" to "`12:59:59`", and starting at BPM IPM1A01.

The twenty three text files must be concatenated into a single text file containing the data for a full day. This can be done using purely linux commands. Here is an example for the day "`2016-08-30`":

```
cat 0830_*_1h_A01.txt > 0830_0000_1d_A01.txt
```

It should be noted that this is simply my naming convention and can be changed at any time. Maybe instead of "`0830_0000_1d_A01.txt`" the file may be named "`test.txt`".

Finally, the text file containing one day's worth of data must be made into a usable ROOT TTree. "`tree_creator.C`" does exactly this. The input is a text file of the form described in Listing (2) and a name for the output ROOT file, and the output is a ROOT file containing a TTree with all of the data from the text file in it. The program needs to be run inside of root, so continuing to use the August 8th example:

```
root -l
.L tree_creator.C
tree_creator("0830_0000_1d_A01.txt", "0830_0000_1d_A01.root")
```

Again, the file can have any name. At this point a usable ROOT TTree has been created! The files needed to be able to collect and analyze data are listed on the following page. The files for download can be found on the accelerator operations computer "`opsl01`" under "`~nowakg/CMBProject`".

- ARC1optics.ele
- IPM1S05_1_IPM1A05_1.ele
- tree_creator.C
- ARC1optics.twi
- IPM1A36_1_IPM1R06_1.cen
- IPM1S05_1_IPM1A05_1.fin
- Arc1SB.lte
- IPM1A36_1_IPM1R06_1.ele
- IPM1S05_1_IPM1A05_1.flr
- ARC2.lte
- IPM1A36_1_IPM1R06_1.fin
- IPM1S05_1_IPM1A05_1.lte
- ARC2optics.ele
- IPM1A36_1_IPM1R06_1.flr
- IPM1S05_1_IPM1A05_1.matr
- calc_ratio_new.C
- IPM1A36_1_IPM1R06_1.lte
- IPM1S05_1_IPM1A05_1.parms
- IPM1A36_1_IPM1R06_1.matr
- IPM1S05_1_IPM1A05_1.sig
- computeXportARC1.pl
- IPM1A36_1_IPM1R06_1.parms
- IPM1S05_1_IPM1A05_1.twi
- computeXportARC2.pl
- IPM1A36_1_IPM1R06_1.sig
- opticsarc1
- eventsarc1
- IPM1A36_1_IPM1R06_1.twi
- quadsARC1.sdds
- getchannels
- IPM1S05_1_IPM1A05_1.cen
- control_script_1d.pl